Forest Ecology and Management 609 (2026) 123650

Contents lists available at ScienceDirect

Forest Ecology and Management

journal homepage: www.elsevier.com/locate/foreco

Higher aboveground carbon stocks at forest edges

Antoine Harel [a,b,c,*], Evelyne Thiffault [a,b], David Paré [c,d], Guillaume Moreau [a,c,e], Alexis Achim [a,b,c], Florence Leduc [a,b,c], Maude Larochelle [f], Yann Chavaillaz [f]

[a] Department of Wood and Forest Sciences, Université Laval, 2405 De la Terrasse Street, Quebec City, Quebec G1V 0A6, Canada
[b] Renewable Materials Research Centre, Université Laval, 2425 De la Terrasse Street, Quebec City, Quebec G1V 0A6, Canada
[c] Centre for Forest Research, Université Laval, 2405 De la Terrasse Street, Quebec City, Quebec G1V 0A6, Canada
[d] Natural Resources Canada, Canadian Forest Service, Laurentian Forestry Centre, 1055 du P.E.P.S, P.O. Box 10380, Stn. Sainte-Foy, Quebec City, Quebec G1V 4C7, Canada
[e] Centre d'études nordiques, Université Laval, 2425 De la Terrasse Street, Quebec City, Quebec G1V 0A6, Canada
[f] Hydro-Québec, Direction Environnement, 800, Boul. de Maisonneuve Est, Montreal, Quebec H2L 4M8, Canada

ARTICLE INFO

Keywords:
Carbon stocks
Aboveground biomass
Stand canopy characteristics
Tree characteristics.
Basal area increment
Edge effect
Powerline right-of-way

ABSTRACT

On a global scale, human activities have significantly fragmented forest landscapes, resulting in over 20% of the remaining forests being located within 100 m of an edge. Forests adjacent to disturbances experience edge effects that can affect aboveground carbon storage through changes in forest structure. Our main objective was to assess aboveground carbon stocks and their drivers at forest edges across a large bioclimatic gradient of upland sites in the temperate and boreal forests of Eastern Canada, using powerline rights-of-way as a case study. We quantified carbon stocks in living and dead trees of all sizes and measured tree growth at stand and tree levels in forests adjacent to powerline rights-of-way. Compared with reference forests (> 50 m from right-of-way), aboveground carbon stocks at forest edges (< 20 m) were up to 60 – 75% higher in boreal spruce forests, 30% higher in temperate forests, but only 2% higher in boreal fir forests. Higher carbon stocks were linked to increased stand density, and thus a higher stand basal area, rather than larger tree diameters. Edge effects on tree characteristics (diameter, total height, crown length and area, and basal area increment) showed no clear pattern and depended on the characteristics of the forest. No edge effect was found in a stand with a recently established right-of-way (less than three years), suggesting that the magnitude of the edge effect varies over time. This study will improve the assessment of the carbon footprint of fragmented forest landscapes.

1. Introduction

Forests play an important role in the global carbon cycle and have represented a global sink of 3.53 ± 0.41 Pg C year^{-1} between 2010 and 2019 (Pan et al., 2024). On a global scale, human activities such as agriculture, urbanization and road network expansion have significantly fragmented forest landscapes (Ma et al., 2023; Riitters et al., 2016), resulting in over 70% of the remaining forests being located within one kilometer of an edge, and 20% within 100 m (Haddad et al., 2015). Forests adjacent to natural or anthropogenic clearings are subject to edge effects (i.e. edge influence) that influence various biotic and abiotic factors, typically extending 10–20 meters from the edge for soil conditions and 25–50 m for aboveground conditions (Schmidt et al., 2017). Although the effect of forest fragmentation on biodiversity loss has been extensively studied (e.g. Pfeifer et al., 2017; Ries et al., 2004; Vanneste et al., 2024; Willmer et al., 2022), the effects of edges on carbon dynamics and stocks remain poorly documented in forest ecosystems (Harper et al., 2015). A recent global study reported that edges have a negative impact on forest aboveground biomass, but the magnitude of this effect (i.e., the strength of the change along the distance gradient) depends on landscape fragmentation and forest cover (Yang et al., 2025).

In temperate ecosystems, previous studies have reported higher aboveground carbon stocks (i.e., the carbon contained in the aboveground biomass of living or dead trees) at forest edges compared with stands located further from the edge (Meeussen et al., 2021b; Morreale et al., 2021; Reinmann and Hutyra, 2017; Remy et al., 2016). The increase in total basal area and thus aboveground biomass at forest edges can be explained by changes at the stand (i.e., increased stand density) and/or at the tree level (i.e., increased individual tree growth) (Smith

* Corresponding author at: Department of Wood and Forest Sciences, Université Laval, 2405 De la Terrasse Street, Quebec City, Quebec G1V 0A6, Canada.
E-mail address: antoine.harel.1@ulaval.ca (A. Harel).

https://doi.org/10.1016/j.foreco.2026.123650
Received 18 November 2025; Received in revised form 20 January 2026; Accepted 25 February 2026

et al., 2018). For example, in European deciduous forests, Meeussen et al. (2020) reported a higher total basal area, stand density and plant area index near forest edges, while stem diameter remained unchanged, suggesting no change in individual tree growth. On the contrary, Reinmann and Hutyra (2017), who documented significantly higher basal area in several temperate broadleaf forest edges, observed that basal area increment (BAI) was constant in forests where stand density (the number of tree stems per unit area) increased near the edge, but BAI was higher when stand density remained stable near the edge. Other studies have also measured an increase in growth at the tree (Briber et al., 2015; McDonald and Urban, 2004) or at the stand level (Chen et al., 1992; Morreale et al., 2021; Reinmann et al., 2020) in temperate or mixed forest edges in the United States. Contrary to the previously cited studies, Ziter et al. (2014) did not observe an edge effect on aboveground carbon stocks in temperate forests of southern Québec (Canada), which they attributed to a compensatory effect between the death of some large trees and the increased productivity of small trees near the edge.

While the dynamics and carbon stocks of forest edges have not been studied to our knowledge in the boreal biome, several studies have documented the structure and diversity of forest edges adjacent to natural or anthropogenic disturbances (Harper et al., 2015, and references therein), and more recently in forests adjacent to oil sand disturbances (seismic lines, well pads, roads, etc.) in Alberta (Canada) (e.g., Boissonneault and Nielsen, 2025; Buss et al., 2024; Jackson et al., 2023). In their meta-analysis, Harper et al. (2015) observed that boreal forest edges were characterized by structural change (lower tree basal area and canopy cover, and greater downed woody debris abundance), but the edge influence was generally weak and did not penetrate very deeply (< 20 m). Also, responses to edge influence vary among edge types, edge ages and forest types (Harper et al., 2015). Boreal forest edges may be more susceptible to damage caused by wind (Yang et al., 2006; Zeng et al., 2009), the speed of which is increased when the landscape is fragmented (Venäläinen et al., 2004) and because of the shallowness of boreal tree root systems (Brassard et al., 2009; Jackson et al., 1996). Higher wind speeds can persist up to one to two tree heights away from the disturbance (Peltola et al., 1999). However, the loss of aboveground carbon in standing trees through windthrow could be offset by increased productivity at forest edges as the availability of growth-limiting factors such as light, water and nutrients (Nemani et al., 2003) may increase for trees near the edge, as suggested by Smith et al. (2018).

Powerline rights-of-way represent a case of man-made linear disturbance in forest landscapes. In the province of Quebec (Canada), where hydropower production is significant, forests are crossed by over 35 000 km of high-voltage powerlines. The powerline rights-of-way, ranging from 30 to 200 meters in width, exhibit distinct characteristics compared to the surrounding forests due to the absence of continuous forest cover and the repeated operations of vegetation control carried out over time. This vegetation control prevents natural edge closure through natural regeneration in the right-of-way (i.e. “edge softening”), thereby artificially maintaining “hard edges” and resulting in a high patch contrast (Esseen et al., 2016; Gascon et al., 2000; Hanson and Stuart, 2005; Harper et al., 2005; Laurance et al., 2009). Apart from edge softening, other mechanisms at work in the forest edge could be edge sealing or edge degradation (Harper et al., 2005). Edge sealing consists of the development of dense vegetation or a lateral canopy of trees in the forest edge, which reduces the penetration of energy into the forest and thus the distance of the edge effect (Harper et al., 2005; Strayer et al., 2003). Conversely, edge degradation, which is well-documented in tropical forests, involves the gradual mortality of trees at the forest edge due to changes in microclimate (higher temperature, lower humidity), increased light availability and lateral wind exposure (Gascon et al., 2000; Laurance et al., 1997). Previous research has shown that microclimate and soil CO_2 and CH_4 effluxes differ in powerline rights-of-way and forest edges compared to undisturbed forests (Harel et al., 2025).

In this study, we used a latitudinal gradient ranging from the temperate Northern Hardwood Forest zones to the northern limit of the closed boreal forest in Northeastern North America to (1) determine whether the edge has an impact on the aboveground carbon stocks contained in large and small living or dead trees in neighboring forests, and (2) identify the mechanisms at the tree and stand levels that affect these carbon stocks over several decades. Such information is needed to validate current carbon accounting methodologies and prevent potential bias in aboveground biomass carbon stock estimations.

2. Materials and methods

2.1. Study area

The study took place in Québec, in eastern Canada (Fig. 1). Seven research sites were selected in three bioclimatic domains, including the north-western part of the spruce-moss domain (*Picea mariana* (Mill.) BSP, sites: NEH-01 and NEM-01), the eastern and northeastern part of the balsam fir-white birch domain (*Abies balsamea* (L.) Mill.; *Betula papyrifera* Marshall, sites: FMA-01, FMA-02 and BAY-01, respectively) and the sugar maple-yellow birch domain (*Acer saccharum*, Marsh.; *Betula alleghaniensis*, Britt., sites: GIM-01 and GIN-02) (Saucier et al., 2009) (Fig. 1). Each research site was established in an upland forest with mesic drainage and structure and composition that are representative of the regional forest landscape. Each site was also crossed by a powerline and its right-of-way. We selected sites where the powerline is oriented approximately north-south since this is the case for most powerlines in Québec (60 – 70%) (Fig. 1) and to limit the effect of this variable on our measurements. Indeed, previous research has shown that the edge aspect is an important factor influencing the magnitude of the edge effect (e.g., Boissonneault and Nielsen, 2025; Eldegard et al., 2015; Smith et al., 2018). We also considered the width of the right-of-way during site selection, taking rights-of-way with widths representative of existing powerlines in the region. Rights-of-way are wider in northern Québec and narrower in southern Québec, especially near cities. Finally, all sites comprised mature forests with no sign of recent natural or anthropogenic disturbance. Each site therefore represented a rectangle measuring 200 m (along the right-of-way) by 100 m (perpendicular to the right-of-way) (Supplementary material).

We grouped our seven study sites into five ecological-climatic clusters based on their similarity in climate, vegetation, and ecological conditions (Table 1). For the two clusters in the eastern maple-yellow birch, the terms “young” and “old” refer to the age of the right-of-way: “young” corresponds to a right-of-way that was established in 2021 (i.e., 2–4 years before the measurements) and “old” corresponds to an older right-of-way (i.e., established 48–50 years before the measurements) (Table 1).

2.2. Experimental design and data collection

2.2.1. Study tree

At each research site, 20–25 study trees were selected near the edge according to their distance from the right-of-way: 5 trees at 0 m from the right-of-way, 10 trees between 2 and 25 m from the right-of-way and 10 trees between 50 and 70 m from the right-of-way, in what we consider to be the reference forest (i.e. control forest) since we assumed that the edge effect would be absent after 50 m (Harper et al., 2015, 2024a) (Fig. 2). Considering the distance gradient described above, trees were randomly distributed to maximize spatial variability within the rectangle defining the study site (Supplementary material). All study trees were live, dominant or co-dominant trees with a diameter at breast height (DBH, 1.3 m) greater than 9 cm. For each tree, the DBH was measured parallel and perpendicular to the right-of-way, and the average of these two measurements was calculated. The height of the tree and of the lowest living branches were measured using a clinometer. The length of the living crown was calculated by subtracting the height of the lowest living branches from the total height. We also calculated

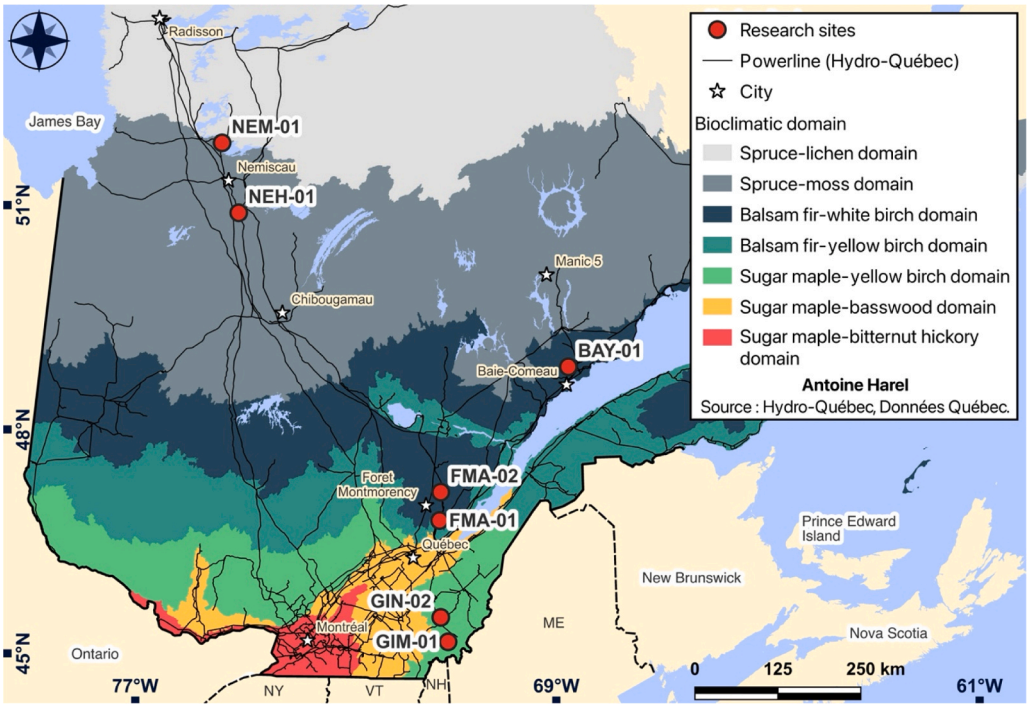

Fig. 1. Location of the eight research sites across the powerline network of Québec (Canada).

the tree live crown projection area onto a horizontal plane in m^2 (S) using the length of four live branches measured in the cardinal directions: north, south, east, and west, based on Eq. 1 (Désaulniers, 1998):

$$S = \frac{1}{4}\sum_{i=1}^{n}\theta_i\left(r_i^2 + r_{i+1}^2\right) \quad (1)$$

where n is the number of branch length measurements (r_i in m) and θ_I is the angle between two successive branches (in radians).

The slenderness coefficient, which is commonly used as an index of a tree resistance to wind-induced stimuli or risk of snow breakage (Albrecht et al., 2012; Skrzyszewski and Pach, 2020; Wang et al., 1998), was calculated for each study tree as the ratio of total height to its DBH (Eq. 2) (Wang et al., 1998):

$$\textit{Slenderness coefficient} = \frac{H}{DBH} \quad (2)$$

where H is the total height of the tree in m and DBH is the diameter at breast height (1.3 m) in m.

For each study tree, two increment cores were collected using a Pressler probe at a height of 1.3 m during the summers of 2023, 2024, and 2025. The two increment cores were perpendicular to the right-of-way, on either side of the tree.

All measurements described above were taken on a total of 174 study trees. Construction work on the GIN-02 research site led to the widening of the right-of-way in 2023, resulting in the loss of 14 study trees from the forest edge.

2.2.2. Stand-level biomass

The aboveground carbon stock contained in large (DBH $\geq$ 9 cm) and small (1 $\leq$ DBH $<$ 9 cm) living and dead trees was quantified using standard forest inventory practices. Around each study tree, a forest inventory was conducted within a 400 m^2 circular plot (radius = 11.28 m). In this plot, all large trees were surveyed (DBH, species, living or dead). The small trees were surveyed (species, living or dead) in a 50 m^2 circular plot (radius = 3.99 m), also centered on the study trees. As mentioned previously, construction work on the GIN-02 site prevented us from completing all inventory plots; 154 plots (for large trees) and 152 plots (for small trees) were completed at the end.

The aboveground biomass (in Mg ha^{-1}) of all living or dead trees present in these plots was calculated using the equations of Lambert et al. (2005), which uses species-specific parameters to calculate aboveground dry biomass (wood, bark, foliage and branches) from DBH. The living or dead aboveground biomass was converted into carbon stock (Mg C ha^{-1}) assuming 0.50 Mg of C per Mg of dry biomass (Penman et al., 2003; Russell et al., 2015).

We used the Shannon-Wiener index (Spellerberg and Fedor, 2003) to quantify DBH and species diversity for each plot using Eq. 3 in the vegan R package (2.6–10) (Oksanen et al., 2025). The Shannon-Wiener index (H) is often used to quantify the horizontal structural diversity of forests (e.g., Boucher et al., 2003; Harel et al., 2021; Morgenroth et al., 2020) and is calculated as:

$$H = -\sum_{i=1}^{n} p_i \quad \ln\left(p_i\right) \quad (3)$$

where p_i is the proportion of trees in the i^{th} class (species or diameter) and n is the number of classes (species or diameter). The value of H ranges from 0 (i.e. only one species / diameter class in the plot) to ln(S) where S is the total number of species / diameter classes (i.e. species / 2 cm diameter classes have the same proportion of individuals).

2.2.3. Leaf area index

The detailed methodology for measuring and calculating leaf area index (LAI) values is presented in the Supplementary material. We used two Plant Canopy Analyzer (LAI-2270C) and two fisheye optical sensors (LAI-2250) (LI-COR Inc., Lincoln, Nebraska, USA) to measure light measurements above and below the canopy at the same time, and to calculate the canopy gap fraction (i.e., the fraction of view from beneath the canopy that is not blocked by foliage). Effective plant area index (i.e. LAI measurement that may include non-leafy vegetation) was then deducted by inverting the calculated canopy gap fraction. The File Viewer 2200 software (LI-COR Inc., Lincoln, Nebraska, USA) was used to match the above and below light measurements, to perform the scattering method proposed by Kobayashi et al. (2013) and to calculate the

Table 1
Climate, dominant vegetation and powerline characteristics of research sites.

Bioclimatic sub-domain	Ecological-climatic cluster	Site ID	Latitude, longitude, altitude	Mean annual air temperature (°C) and total annual precipitation (mm)[2]	Growing season length (days)[2]	Mean growing degree-days (4°C)[2]	Surface deposit[3]	Stand structure[4]	Canopy dominant tree species	Powerline characteristics		
										Right-of-way width (m)	Aspect	Year of right-of-way creation
Eastern maple-yellow birch domain	Eastern maple-yellow birch (young right-of-way)	GIM-01	45.56 N 70.70 W, 422 m	4.48 °C 1 166 mm	165	1 861	1 A	Irregular	Trembling aspen (*Populus tremuloides* Michx), Balsam fir (*Abies balsamea* (L.) Mill.), Red maple (*Acer rubrum* L.), White birch (*Betula papyrifera* Marsh.), Balsam poplar (*Populus balsamifera* L.), Largetooth aspen (*Populus grandidentata* Michx.)	40	339° N	2021
	Eastern maple-yellow birch (old right-of-way)	GIN-02	45.73 N 70.18 W, 371 m	4.67 °C 1 251 mm	168	1 913	1 A	Irregular	Balsam fir, Trembling aspen, Sugar maple (*Acer saccharum*, Marsh.), Red spruce (*Picea rubens*, Sarg), White birch, Red maple, Yellow birch (*Betula alleghaniensis*, Britt.)	40	311° NW	1975 and 2024[5]
Eastern balsam fir-white birch domain	Eastern balsam fir-white birch	FMA-01	47.16 N 71.25 W, 598 m	1.16 °C 1 433 mm	129	1 309	1AY	Regular	Balsam fir, White birch	50	53° NE	1959
		FMA-02	47.29 N 71.19 W, 807 m	-0.13 °C 1 428 mm	115	1 105	1 A	Regular	Balsam fir, White birch, White spruce (*Picea glauca* Moench)	50	16° N	1927
	Eastern spruce-moss	BAY-01[1]	49.20 N 68.40 W, 112 m	2.23 °C 1 010 mm	160	1 428	5S	Regular	Black spruce (*Picea mariana* (Mill.) BSP)	120	306° NW	1960
Western spruce-moss domain	Western spruce-moss	NEH-01	51.24 N 75.67 W, 342 m	-0.80 °C 851 mm	127	1 281	1AR	Regular	Jack pine (*Pinus banksiana*, Lamb.), black spruce	160	340° N	1981
		NEM-01	52.16 N 76.14 W, 286 m	-1.43 °C 786 mm	127	1 191	1BA	Regular	Black spruce, Jack pine	60	58° NE	2006

[1] Although the BAY-01 site is located within the eastern balsam fir-white birch domain, it was assigned to the "eastern spruce-moss" cluster due to its forest composition, which was dominated by black spruce.
[2] These data were calculated for the years 1991–2020 using BioSIM (Fortin et al., 2022; Régnière et al., 2017), see Supplementary material for more details.
[3] 1 A: glacial deposit, no specific morphology, undifferentiated till. 1AY: glacial deposit, no specific morphology, undifferentiated till, average thickness 50 cm to 1 m with rare to very rare rock outcrops. 5S: Marine deposit, marine (shallow water facies). 1AR: Thin undifferentiated till. 1BA: Ablation till.
[4] The horizontal structure was assessed by visualizing the distribution of DBH classes in each circular inventory plot.
[5] There are two powerlines in the right-of-way; the right-of-way was widened to allow construction of the second powerline.

effective LAI values. LAI values were computed from the effective plant area index measurements while correcting for the non-random spatial distribution of leaves (needles clumping within the shoot and at a larger scale than the shoot) (Chen, 1996). We took 25 light measurements randomly distributed in the forest edge (between 10 and 30 m from the right-of-way) and another 25 in the reference forest (between 50 and 70 m from the right-of-way) at each site. We carried out this operation a second time, 50 m from the study site, to ensure at least two plots of forest edge and reference forest per site. After computation, the LAI values were averaged for each plot (n = 2 for forest edge and n = 2 for reference forests in each site).

2.3. Dendrochronological measurements

The collected increment cores were glued to wooden blocks, air-dried and then sanded with increasingly finer-grained paper. Annual tree rings were measured using a Velmex micrometer (Velmex Inc., Bloomfield, NY, USA) (±0.002 mm), enabling the construction of a time series of annual ring widths for each core. The raw ring width measurements of the two cores collected on a given study tree were then averaged per year to produce a single annual growth series for each tree.

Statistical cross-dating verification was performed using the COFECHA software (Holmes, 1983) to validate the dating of each tree within

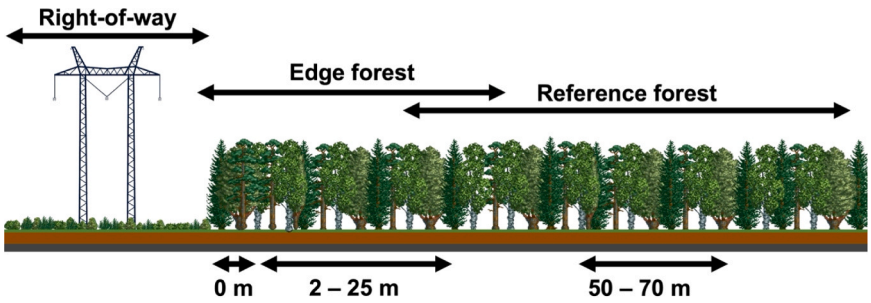

Fig. 2. Layout of study trees at each site. The trees are aligned perpendicular to the power line right-of-way, with trees located zero m from the right-of-way, or between 2 and 25 m or 50 and 75 m from the right-of-way.

the same site and apply corrections if needed. For each site, the expressed population signal (Wigley et al., 1984) was calculated and tree-ring series that exhibited low correlation with others were iteratively removed until the expressed population signal exceeded the threshold of 0.85 (Buras, 2017). For each species and site, a master chronology was constructed from the dated series, and each remaining individual series was visually compared to the master chronology for validation. In total, well-dated average ring-width series were obtained for 154 trees.

Ring widths for each tree were converted to BAI using the pith to bark method when the pith was present in the core, or the bark to pith method when it was not (Biondi, 1999; Visser et al., 2023). Both methods are implemented in the dplR R package (1.7.8) (Bunn, 2008). BAI enables the detection of increases in total biomass growth in a tree, even in the presence of an age-related decline in growth (Phipps and Whiton, 1988).

To assess the impact of right-of-way clearing on BAI, we calculated the percentage growth change (%GC) (Fraver and White, 2005; Nowacki and Abrams, 1997) using the mean BAI for the five years preceding and following the creation of the right-of-way (Eq. 4). Out of the 174 cored trees, only 58 were retained for Eq. 4, as several tree-ring width series did not extend back to the year the right-of-way was cleared. This applied to all trees on sites FMA-01 and FMA-02. Trees from GIM-01 were also excluded because the right-of-way was too recent (created in 2021).

$$\%GC = \frac{BAI_{AFT-5} - BAI_{BEF-5}}{BAI_{BEF-5}} \times 100 \quad (4)$$

where %GC is the percentage growth change between preceding and subsequent five-year means, BAI_{AFT-5} is the mean basal area increment over five years following the creation of the right-of-way (mm^2) and BAI_{BEF-5} is the mean basal area increment over five years preceding the creation of the right-of-way (mm^2).

2.4. Statistical analyses

Linear mixed models (LMMs) (Zuur et al., 2009) were used to test the hypothesis that the edge effect had an impact on aboveground carbon stocks, stand and tree variables. First, we built different LMMs for aboveground carbon stocks contained in all trees, large living trees, small living trees, large dead trees, and small dead trees, as well as models for stand-level variables (basal area, stand density, mean DBH, DBH class diversity and species diversity) using the nlme R package (3.1–168) (Pinheiro et al., 2017). For these models, distance from the right-of-way (continuous variable), ecological-climatic clusters (categorical variable, 5 levels: sugar maple-yellow birch forests with a young or an old right-of-way, western and eastern boreal spruce-moss forests and eastern balsam fir-white birch forests; Table 1) and their interaction were used as fixed factors. The site was used as a random factor. A specific variance structure was used for each level of the ecological-climatic cluster. A similar model was used for LAI, with the difference that distance was treated as a categorical factor (two levels: forest edges or reference forest), since LAI measurements were collected at forest edge (10 – 30 m from the right-of-way) and reference forests (50 – 70 m from the right-of-way) regardless of distance from the right-of-way. In a subsequent step, we built LMMs for tree-level variables (DBH, total height, crown height, crown projection area and slenderness coefficient) with the lme4 R package (1.1–37) (Bates et al., 2015), using distance from the right-of-way (continuous variable), ecological-climatic cluster (categorical variable, 5 levels: the same as listed above) and their interaction as fixed factors. The models included two random intercepts to account for variability associated with the site and the species of the study tree. Finally, we built an LMM for the percentage growth change (%GC) with the lme4 R package, using distance from the right-of-way (continuous variable), ecological-climatic cluster (categorical variable, 5 levels: the same as listed above) and their interaction as fixed factors; the site was used as a random factor.

For all models, the normality and homoscedasticity of the model residuals were visually checked using a standard graphical approach, as well as with the performance (0.10.8) (Lüdecke et al., 2021) and DHARMa (0.4.6) (Hartig, 2022) R packages. Logarithmic transformations were performed to meet residual normality assumptions when necessary. The restricted maximum likelihood method was used to obtain an unbiased estimate of the variance components (fixed factors) (West et al., 2006). Joint tests of contrasts or type III F-tests (Satterthwaite adjustment for the denominator degrees of freedom) among each term in the model were computed for the significance of fixed effects (distance from the right-of-way, ecological-climatic cluster and their interaction) using the lmerTest R package (3.1–3) (Kuznetsova et al., 2017) or the emmeans R package (1.11.0) (Lenth et al., 2024). The percentage of variance explained by the fixed effects relative to the overall variance (R^2 marginal, R^2_{mar}) and by the random and fixed effects (R^2 conditional, R^2_{con}) was calculated based on Nakagawa et al. (2017) with the MuMIn R package (1.47.5) (Bartoń, 2024). For the visual representation of the model, we calculated the estimated marginal means (EMM) (Searle et al., 1980) for the model fixed factors (distance from the right-of-way for each level of the ecological-climatic cluster) using the containment or Kenward-Roger method for degrees of freedom with the emmeans R package.

We performed all modelling and statistical analyses in R (4.3.2) (R Core Team, 2020). Data wrangling and graphs were produced using the dplyr (1.1.4) and ggplot2 (3.5.1) R packages, respectively (Wickham et al., 2023, 2020). $\alpha < 0.05$ was used as the threshold for significance for all analyses.

3. Results

3.1. Aboveground carbon stocks at forest edge

Sugar maple-yellow birch forests (sites GIM-01 and GIN-02) exhibited generally higher aboveground carbon stocks contained in the aboveground biomass of all trees (large and small living or dead trees)

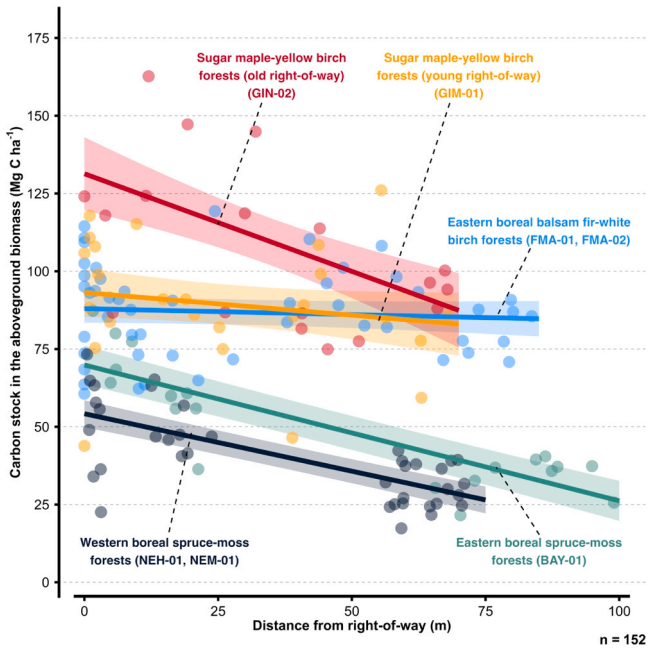

Fig. 3. Estimated marginal means (EMM) for carbon stocks contained in large and small living or dead trees aboveground biomass (ABGC, DBH ≥ 9.0 cm) as a function of distance from the rights-of-way for each climatic-ecological cluster. Site IDs are shown in labels. The line represents the EMM, the shaded area represents the confidence interval (95%), the points are the raw values used for the model and n is the number of plots where ABGC was measured.

than eastern boreal balsam fir-white birch forests (sites FMA-01 and FMA-02), which in turn contained higher aboveground carbon stocks than spruce-moss forests (sites NEH-01, NEM-01 and BAY-01) (Fig. 3). Overall, the distance from the right-of-way had a significant negative effect on carbon stocks ($F_{(1,140)} = 23.31$, $\mathbf{p = <0.001}$) ($R^2_{mar} = 0.84$, $R^2_{con} = 0.87$). The ecological-climatic cluster ($F_{(4,2)} = 28.59$, $\mathbf{p = 0.034}$), and its interaction with distance from the right-of-way ($F_{(4,140)} = 5.47$, $\mathbf{p = <0.001}$), both had significant effects on aboveground carbon stocks, indicating that the rate of carbon stock variation with distance (i.e. the magnitude of the edge effect) depended on the ecological-climatic cluster. The slope was similar in the western and eastern boreal spruce-moss forests and the sugar maple-yellow birch forests with an old right-of-way, while it neared zero in the sugar maple-yellow birch forest edges with a young right-of-way and the eastern boreal balsam fir-white birch forest edges (Fig. 3). Compared to reference forests (> 50 m from the right-of-way), the aboveground carbon stock of trees at forest edges (< 20 m from the right-of-way) was 62.37% higher for the western boreal spruce-moss forests, 76.54% higher for the eastern boreal spruce-moss forests and 33.49% higher for the sugar maple-yellow birch forests with an old right-of-way. For the sugar maple-yellow birch forest edges with a young right-of-way and for the eastern boreal balsam fir-white birch forest edges, the increases were only 8.59% and 2.57%, respectively. Detailed information on carbon stocks contained in aboveground biomass is presented in the Supplementary material.

Looking more closely at the different types of trees contributing to the carbon stocks, the carbon stocks in both large living trees and small living trees were significantly higher closer to the edge, while distance from the right-of-way had no significant effect on carbon stocks contained in small dead trees (Table 2, Fig. 4). Although the distance from the right-of-way had no significant main effect on the carbon stock of large dead trees, the significant interaction between the distance and the ecological-climatic cluster implies that the effect of distance depends on the ecological-climatic cluster (Table 2). The edge effect on the carbon stock of large dead trees was negligible in all ecological-climatic clusters except in the eastern boreal spruce-moss forests, where it was 132.82% higher at the forest edge (mean: 492 (sd: 176) large dead trees/ha) than in the reference forest (mean: 118 (sd: 59) large dead trees/ha) (Supplementary material). On average, large trees (living or dead) held 98.24% (sd: 1.57%) of the carbon stock contained in aboveground tree biomass, while living trees (large and small) held 86.96% (sd: 10.50%) of the carbon stock.

3.2. Stand characteristics at forest edge

The stand basal area and stand density were significantly higher near the right-of-way, but the magnitude of the edge effect varied among the ecological-climatic clusters (Table 3, Fig. 5). Both basal area and stand density were up to 45% higher in the edge (< 20 m from the right-of-way) relative to reference forests (> 50 m from the right-of-way) in the western and eastern boreal spruce-moss forests and in the sugar maple-yellow birch forests with an old right-of-way, but only 6% higher in the eastern boreal balsam fir-white birch forests and the sugar maple-yellow birch forests with the young right-of-way (exact values are presented in Supplementary material). The average tree DBH did not vary with distance from the right-of-way (Table 3). Neither the distance from the right-of-way nor the ecological-climatic cluster had a significant main effect on the DHB class diversity or species diversity (Table 3). However, in both cases, their interaction was significant, indicating that the effect of distance varied among ecological-climatic clusters (Supplementary material). In both cases, only the eastern boreal spruce-moss forests stood out in terms of higher DBH class and species diversity at the forest edge than in the reference forest, while this was negligible in the other clusters (Supplementary material). In the eastern boreal spruce-moss forests, the forest edge consisted of two species (black

Table 2
Linear mixed model significance test results for the fixed effect for the carbon stock contained in large living trees, small living trees, large dead trees and small dead trees (large living and dead trees, with DBH > 9.0 cm). Each column represents a specific model. Significant results are in bold.

	Join tests of contrasts among each term in the model[1] Carbon stocks contained in:			
	Large living trees	Small living trees	Large dead trees	Small dead trees
Distance from the right-of-way	F(1, 142.0) = 14.32, **p < 0.001**	F(1, 140.0) = 18.87, **p < 0.001**	F(1, 142.0) = 3.74, p = 0.055	F(1, 140.0) = 1.26, p = 0.264
Ecological-climatic cluster[2]	F(4, 2.0) = 23.09, **p = 0.042**	F(4, 2.0) = 11.07, p = 0.085	F(4, 2.0) = 2.83, p = 0.278	F(4, 2.0) = 0.36, p = 0.822
Interaction between distance and cluster	F(4, 142.0) = 3.44, **p = 0.010**	F(4, 140.0) = 5.42, **p < 0.001**	F(4, 142.0) = 7.68, **p < 0.001**	F(4, 140.0) = 1.90, p = 0.114
R_{mar}[3]	0.82	0.41	0.59	0.13
R_{con}[3]	0.85	0.41	0.88	0.70

[1] F(degrees of freedom in the numerator, degrees of freedom in the denominator).
[2] Sugar maple-yellow birch forests (young and old right-of-way), eastern balsam fir-white birch forests, western and eastern boreal spruce-moss forests.
[3] R^2_{mar} measures the variance explained by fixed effects, while R^2_{con} includes both fixed and random effects.

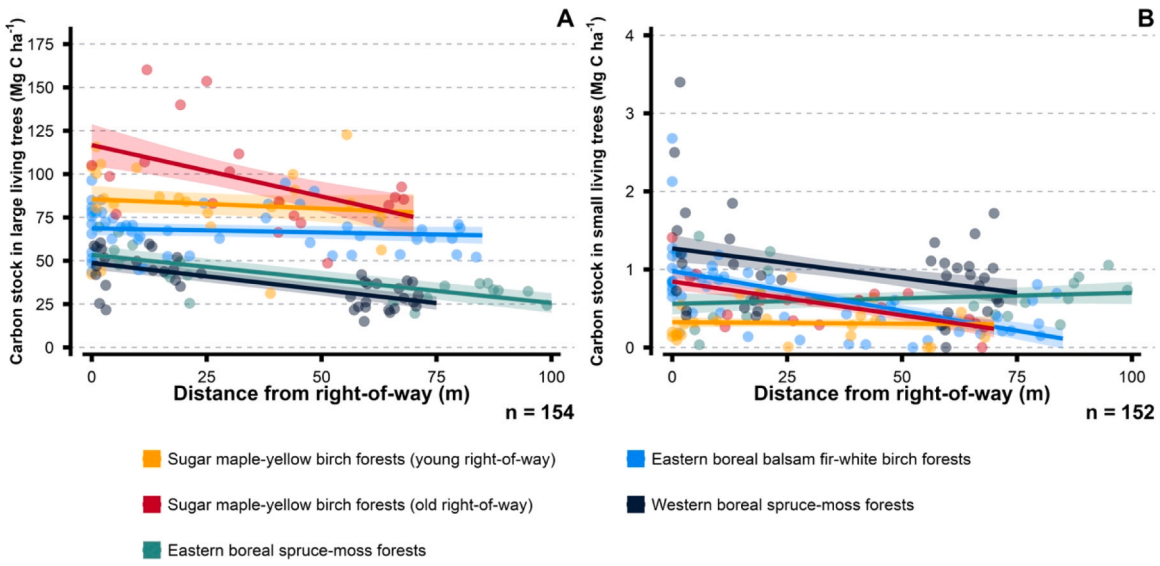

Fig. 4. Estimated marginal means (EMM) for the carbon stocks contained in large living trees aboveground biomass (ABGC, DBH ≥ 9.0 cm) (A) and in small living trees aboveground biomass (DBH < 9.0 cm) (B) as a function of distance from the rights-of-way for each ecological-climatic cluster. The line represents the EMM, the shaded area represents the confidence interval (95%), the points are the raw values used for the mode and n is the number of plots where the variables were measured.

Table 3
Linear mixed model significance test results for the fixed effect for basal area, stand density, mean DBH and DBH and species Shannon diversity index (all trees with DBH > 9.0 cm). Each column represents a specific model. Significant results are in bold.

	Join tests of contrasts among each term in the model[1]				
	Basal area	Stand density	Mean DBH	DBH diversity[2]	Species diversity[2]
Distance from the right-of-way	F(1, 142.0) = 36.41, **p < 0.001**	F(1, 142.0) = 53.31, **p < 0.001**	F(1, 145.0) = 1.09, p = 0.298	F(1, 142.0) = 1.68, p = 0.198	F(1, 142.0) = 0.04, p = 0.834
Ecological-climatic cluster[3]	F(4, 2.0) = 6.65, p = 0.135	F(4, 2.0) = 0.98, p = 0.561	F(4, 2.0) = 15.84, p = 0.060	F(4, 2.0) = 13.99, p = 0.068	F(4, 2.0) = 8.45, p = 0.109
Interaction between distance and cluster	F(4, 142.0) = 4.33, **p = 0.002**	F(4, 142.0) = 6.22, **p < 0.001**	F(4, 145.0) = 1.08, p = 0.366	F(4, 142.0) = 5.45, **p < 0.001**	F(4, 142.0) = 21.36, **p < 0.001**
R_{mar}[4]	0.70	0.35	0.89	0.84	0.84
R_{con}[4]	0.83	0.77	0.96	0.94	0.98

[1] F(degrees of freedom in the numerator, degrees of freedom in the denominator).
[2] Shannon diversity index.
[3] Sugar maple-yellow birch forests (young and old rights-of-way), eastern balsam fir-white birch forests, western and eastern boreal spruce-moss forests.
[4] R^2_{mar} measures the variance explained by fixed effects, while R^2_{con} includes both fixed and random effects.

spruce and balsam fir) with DBH ranging from 10 to 32 cm, while the reference forest consisted only of black spruce ranging in size from 10 to 24 cm (Supplementary material). Finally, LAI was not significantly different between 10 – 30 m and 50 – 70 m from the right-of-way ($F_{(1,15)}$ = 1.06, p = 0.319, R^2_{MAR}: 0.60, R^2_{CON}: 0.60). Details for the LAI variables and stand variable can be found in the Supplementary material section, respectively.

3.3. Tree characteristics at forest edge

Distance from the right-of-way had no significant positive or negative effect on tree DBH or slenderness coefficient (Table 4). Neither distance from the right-of-way nor the ecological-climatic cluster had a significant main effect on total height or the crown height (Table 4). However, their interaction was significant (Table 4), indicating that the effect of distance varied among the ecological-climatic clusters (Supplementary material). The greatest difference in crown length occurred in the eastern balsam fir-white birch forests, where the trees directly on the edge had a living crown height that averaged 14.91 m (sd: 5.58 m, 82.42% of total tree height), compared to 6.69 m (sd: 3.05 m, 40.65% of total tree height) in the reference forest (> 50 m from the right-of-way). For total height, the greatest difference was observed in the sugar maple-yellow birch forests with an old right-of-way, where trees at the forest edge were 19.80% shorter than those in the reference forest. Finally, the crown projection area of the study trees was significantly lower at the forest edge compared to the reference forest (Table 4, Supplementary material). The crown projection area of study trees at the forest edge (< 20 m from the right-of-way) was from 10 and 30% smaller than that of trees in the reference forest (> 50 m from the right-of-way) in both the eastern and western boreal spruce-moss forests and the sugar maple-yellow birch forests with an old right-of-way. Detailed information on the study tree variables (values, visualization of model results, etc.) is also presented in the Supplementary material.

No significant main effects of either distance from the right-of-way or ecological-climatic cluster were observed on %GC within the five years following rights-of-way establishment, but their interaction was significant (Table 4), suggesting that the effect of distance differed among ecological-climatic clusters (Supplementary material). The variation in %GC according to the distance from the right-of-way was negligible in the sugar maple-yellow birch forests with an old right-of-way and the

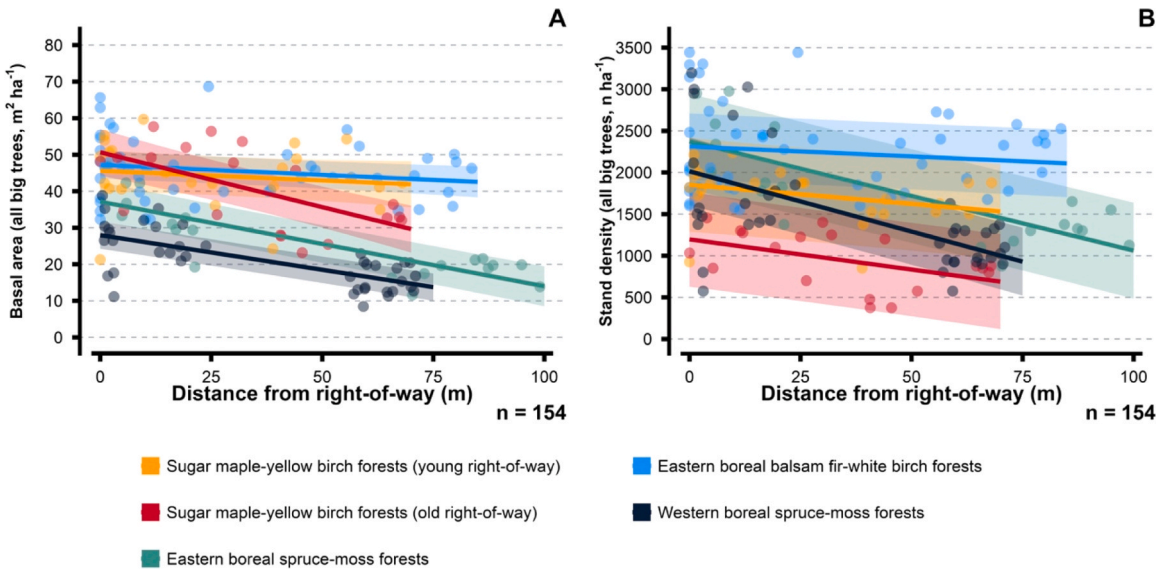

Fig. 5. Estimated marginal means (EMM) for the basal area (A) and stand density (B) (all trees with DBH > 9.0 cm) as a function of distance from the rights-of-way for each ecological-climatic cluster. The line represents the EMM, the shaded area represents the confidence interval (95%), the points are the raw values used for the mode and n is the number of plots where the variables were measured.

Table 4
Linear mixed model significance test results for the fixed effect for diameter at breast height, total height, crown length, crown projection area, slenderness coefficient and percentage growth change (%GC) within the five years following the right-of-way creation. Each column represents a specific model. Significant results are in bold.

	Join tests of contrasts among each term in the model[1]					
	Diameter at breast height	Total height	Crown length	Crown projection area	Slenderness coefficient	%GC
Distance	F(1, 155.6) = 0.51, p = 0.478	F(1, 145.4) = 0.48, p = 0.489	F(1, 145.3) = 0.12, p = 0.726	F(1, 140.5) = 5.77, **p = 0.018**	F(1, 148.2) = 0.03, p = 0.873	F(1, 51.3) = 3.46, p = 0.068
Ecological-climatic cluster[2]	F(4, 3.8) = 2.55, p = 0.199	F(4, 3.4) = 1.90, p = 0.297	F(4, 3.6) = 0.44, p = 0.777	F(4, 4.2) = 4.41, p = 0.083	F(4, 31.2) = 0.79, p = 0.542	F(2, 2.0) = 4.22, p = 0.192
Interaction between distance and cluster	F(4, 152.8) = 0.95, p = 0.435	F(4, 142.8) = 3.54, **p = 0.009**	F(4, 141.3) = 3.83, **p = 0.005**	F(4, 138.4) = 2.07, p = 0.088	F(4, 144.4) = 1.30, p = 0.274	F(2, 51.3) = 9.59, **p = <0.001**
R_{mar}[3]	0.35	0.35	0.14	0.52	0.06	0.21
R_{con}[3]	0.69	0.70	0.29	0.83	0.42	0.53

[1] F(degrees of freedom in the numerator, degrees of freedom in the denominator).
[2] Sugar maple-yellow birch forests (young and old right-of-way), eastern balsam fir-white birch forests, eastern boreal spruce-moss forests, western boreal spruce-moss forests and eastern boreal spruce-moss forests.
[3] R^2_{mar} measures the variance explained by fixed effects, while R^2_{con} includes both fixed and random effects.

western boreal spruce-moss forests, whereas in the eastern boreal spruce-moss forests, trees located at the edge had an average %GC of 111.86% (sd: 10.98%), compared to 21.55% (sd: 23.04%) in the reference forest. The mean [5th – 95th interval] cumulative basal area increments over five years before and after the right-of-way clearing were 437 mm^2 [54 – 1514] and 486 mm^2 [72 – 1447], respectively (n = 58 study trees).

4. Discussion

We measured higher carbon stocks in the aboveground biomass of trees in forests at the edge of powerline rights-of-way compared with more distant forests. While a general trend was observed when including all sites, the results indicated that the magnitude of the edge effect varied depending on the climatic and ecological conditions of the site and was dynamic over time.

4.1. Aboveground carbon stocks

At forest edges, higher carbon stocks in the aboveground biomass of large trees were mainly driven by increased stand density, and thus higher total basal area, rather than by individually larger tree diameters. This phenomenon had also been observed previously in temperate forest edges in Europe (Meeussen et al., 2020, 2021b) and the United States (Morreale et al., 2021; Reinmann and Hutyra, 2017). Higher stand density near linear disturbances had also been observed in boreal forests (Boissonneault and Nielsen, 2025; Jackson et al., 2023). The productivity of forest edges may be enhanced by favourable light and microclimatic conditions (McDonald and Urban, 2004; Meeussen et al., 2021a; Mourelle et al., 2001; Schmidt et al., 2017) or by increased nitrogen atmospheric deposition (De Schrijver et al., 2007; Meeussen et al., 2021b; Remy et al., 2018b, 2018a; Weathers et al., 2001; Wuyts et al., 2009). In contrast to the findings of Ziter et al. (2014) in temperate forests comparable to our most southern sites but in a landscape dominated by agriculture, we did not observe increased mortality among small and large trees at forest edges. Instead, our results suggest that more favourable conditions in the edges compared with reference areas (beyond the influence of the clearing) allowed a greater number of small trees to survive and reach maturity near the right-of-way. This difference could also be explained by a landscape less dominated by agriculture

(Yang et al., 2025) and overall lower levels of human disturbance. Only one of our five sites (BAY-01) located in the boreal forest showed an increase in the mortality of large trees at the forest edge compared to the reference forest. However, this phenomenon was not widespread enough to counteract the effect of the greater density of large and small living trees on carbon stocks. This site is also the only one where the forest edge had a higher diversity of tree diameters compared with the reference forest. Our results also differ from those of Yang et al. (2025) who reported a negative edge effect on forest aboveground biomass at the global scale. While large-scale remote sensing studies provide crucial data on carbon stock losses associated with forest fragmentation at the global scale, fine-scale studies based on empirical data remain necessary to identify the mechanisms explaining the magnitude and distance of the edge effect on carbon stocks. This is especially true in the boreal forest, where there is a significant lack of empirical data, and where edge effects likely do not extend far into the forest (Harper et al., 2024b, 2015, 2005, 2004), making them difficult to detect with 30-m resolution pixels derived from satellite Earth observation data (Hansen et al., 2013; Harris et al., 2021).

4.2. Dynamic structural variation at forest edges

The magnitude of the edge effect was comparable between forests located in boreal spruce-moss forests and old sugar maple-yellow birch forests. Our results, based on comparisons between plots located less than 20 m and those more than 50 m from the right-of-way, suggest that edge effects in boreal spruce-moss forests extend to at least 20 m, which falls within (albeit at the upper end) of the 5 – 20 m range reported in previous studies (Braithwaite and Mallik, 2012; Harper et al., 2024a, 2015, 2004). However, the distance of the edge effect likely depends on the characteristics of the disturbance (size and type), and therefore on the contrast patch (Esseen et al., 2016; Harper et al., 2005). In other studies, the distance of the edge effect was evaluated in an area that extends up to 40 m for disturbances of similar size and type (seismic lines and roads in oil sands disturbances) (Jackson et al., 2023). Further research is needed to quantify the distance of edge influence more precisely. A similar methodological design, with fewer plots per transect placed at fixed distances and extending beyond 70 m, could provide a practical option for future research aimed at better quantifying the extent of edge influence.

In contrast to our other sites, the edge effect on aboveground carbon stocks was negligible in the sugar maple-yellow birch forests with a young right-of-way and the eastern balsam fir-white birch forests. In the first case, this is likely because the right-of-way was cleared only two to three years before the measurements were taken. This suggests that the magnitude of the edge effect varies over time and that the forest structure has not yet been significantly impacted by the new disturbance. For our eastern balsam fir-white birch forests, several hypotheses may explain why the edge effect is weak or undetectable, including: (1) both studied rights-of-way are relatively old (66 and 96 years), and the forest stands are composed of mature balsam fir trees of approximately 50 years of age, meaning they were not present when the rights-of-way were cleared. Conversely, this could also explain the lack of observed mortality (such as windthrow gaps) at the forest edge, as the forest had already recovered. (2) edge sealing through lateral foliage expansion of trees along the edge could have reduced the amount of light energy penetrating the forest (e.g. Mourelle et al., 2001), thereby reducing the distance and magnitude of edge effect (Strayer et al., 2003). Indeed, in the eastern balsam fir-white birch forests, trees located directly on the edge had, on average, twice the living crown height of those in the reference forest. Our hypothesis is that the advanced age of the powerline has allowed balsam firs, a shade-tolerant species that responds to increased light availability following minor disturbances (Prévost et al., 2016), to develop vertical foliage along their stems. Because edge influence originates from only one side, trees located directly at the edge benefited from increased light availability and thereby buffered the edge effect.

4.3. Tree characteristics in edges

The distances from the right-of-way had no significant impact on average tree DBH or slenderness coefficient. The crown projection area was reduced at forest edges, which is consistent with the higher stand density that we observed near the right-of-way (Li et al., 2022; Thorpe et al., 2010). Except for sites in boreal balsam fir forests, trees near the right-of-way did not have longer crowns than those located further away. One possible explanation is that the creation of the right-of-way favoured the growth of small trees, whose crowns occupied the newly available space (i.e., edge sealing), preventing the mature trees from spreading their crowns downward.

We did not detect any changes in individual tree BAI for trees near the edge compared to those further away in the five years immediately following the right-of-way clearing in the western eastern boreal spruce-moss forests and the sugar maple-yellow birch forests with an old right-of-way. This is consistent with our observation that we did not detect any difference in DBH between cored trees near the edge and those in the reference forest. However, this result is not consistent with previous studies that showed an increased growth at the tree or stand level following disturbance in temperate or mixed forest edges in the United States (Bowering et al., 2006; Briber et al., 2015; Chen et al., 1992; McDonald and Urban, 2004), in particular in early-successional species with high maximum photosynthetic rates (McDonald and Urban, 2004). Nevertheless, our results are comparable to those of (Reinmann and Hutyra, 2017), who observed, in some cases, no change in individual tree growth with distance from the edge in forests, while stand density increased near the edge. In other cases, they observed forest edges with stem densities comparable to those of interior forests, yet individual trees displayed higher growth rates at the edge (Reinmann and Hutyra, 2017). Nonetheless, at one site located in the eastern boreal spruce–moss forest, some black spruce trees (which were around 40 years old at the time the right-of-way was created) displayed enhanced radial growth within five years of right-of-way establishment. Since a positive growth response following canopy opening can depend on several cofounding factors, such as tree age, diameter, crown size and position, prior growth rate, species and health (Black and Abrams, 2003a, 2004b), it is difficult to identify a clear pattern due to the limited number of study sites. By focusing solely on dominant and co-dominant trees, our study excludes the growth responses of trees that were saplings or suppressed at the time of the right-of-way's creation, which may have benefited more from its creation. In any case, we did not detect any edge effect on tree size (both the DBH of the study trees and the mean DBH of the inventory plots).

5. Conclusion

We documented aboveground carbon stocks contained in large and small living or dead trees and various variables at the stand (basal area, stand density, mean diameter, diameter and species diversity) and tree levels (diameter, total height, crown height, crown projection area and basal area increment). Aboveground carbon stocks at forest edges were up to 62.37% and 76.54% higher in western and eastern boreal spruce-moss forests, respectively, 33.49% higher in the sugar maple-yellow birch forest with an old right-of-way, and only 2.57% in the eastern boreal balsam fir-white birch forest edge. Less than three years after the right-of-way was cleared, carbon stocks were only 8.59% higher in the sugar maple-yellow birch forest edge. Higher carbon stocks were associated with higher stand density, and thus with a higher total basal area, rather than larger tree diameters. In boreal fir forests, edge sealing may have reduced light availability, thereby mitigating edge effects and resulting in similar conditions between edge and interior forests. The edge effect on tree characteristics (diameter, height, crown height, and basal area increment within the five years following rights-of-way

establishment) varied depending on forest attributes, showing no consistent pattern.

The results presented here represent a first step in quantifying the biogenic carbon footprint of linear disturbances, such as those created by power grids. Indeed, the quantification of emissions associated with the deployment of electricity transmission lines has typically not been based on detailed field measurements (e.g., Levasseur et al., 2021). We have already shown that soil CO_2 effluxes were higher in forests adjacent to powerline rights-of-way, suggesting differences in the structure and productivity of forest edges (Harel et al., 2025). Here, we observed that forests adjacent to rights-of-way contain more carbon in their aboveground tree biomass than more distant forests, particularly at our research sites located in temperate and boreal spruce forests. Whether this additional carbon is sufficient to offset the carbon loss associated with the clearing of the powerline right-of-way remains to be assessed. Variables such as the width and orientation of the right-of-way, characteristics of vegetation within the right-of-way, and ecological conditions of the forest (age, species, density, forest health, etc.) will require special consideration. For example, edge effects on microclimate and light intensity were generally stronger at south- and west-facing forest edges (Franklin et al., 2021). Further research will be required to quantify the magnitude and distance of the edge effect across different sites and ecosystems, particularly in mixed forests. Finally, it will be necessary to document vegetation dynamics over time following right-of-way creation (i.e., patterns of mortality, growth, and regeneration), for example by using a chronosequence from a comparable site. As described above, a methodology that uses fewer plots but at fixed distances between sites would be relevant, particularly because it would allow the distance and magnitude of the edge effect to be more precisely estimated (Harper et al., 2005; Harper and Macdonald, 2011). Remote sensing techniques offer a powerful method to quantify the magnitude, distance, and estimates of aboveground carbon stocks at the landscape scale.

CRediT authorship contribution statement

Evelyne Thiffault: Writing – review & editing, Supervision, Project administration, Funding acquisition, Conceptualization. **Antoine Harel:** Writing – review & editing, Writing – original draft, Methodology, Investigation, Formal analysis, Data curation, Conceptualization. **Yann Chavaillaz:** Writing – review & editing. **Maude Larochelle:** Writing – review & editing, Project administration. **Florence Leduc:** Writing – review & editing, Formal analysis. **Guillaume Moreau:** Writing – review & editing, Supervision. **Alexis Achim:** Writing – review & editing, Supervision. **David Paré:** Writing – review & editing, Supervision, Conceptualization.

Declaration of Competing Interest

The study was funded with a NSERC-Alliance grant from the Government of Canada in partnership with Hydro-Québec. Hydro-Québec is the public utility responsible for the generation, transmission and distribution of electricity in Quebec (Canada). M. Larochelle and Y. Chavaillaz are employees of Hydro-Québec. The other authors declare that they have no competing financial interests or personal relationships that could have influenced the work reported in this paper.

Acknowledgement

The authors would like to thank Madeleine Prudhommeaux, José-Gabriel Yee Paré, Renée Hudon, Salomé Chamorro-Godin, Estelle Estrugo, Kevin Martin, Marie-Anne Michaud-Valcourt, Jérémy Duchesne Pomerleau, Annabelle Poulin, Dorianne Desrochers, Jean Bernier, Valentin Beaufils, Étienne Paradis, Kimberley Boyle, Francis Nadeau, Rosalie Côté, Gaspard Hutteau d'Origny, Michelle Rousselle and Alexandre Côté for their contribution to the fieldwork. We would also like to thank Ann Delwaid, Emmanuelle Baby-Bouchard, Catherine Chagnon, Flavie Dube and Vicky Martin for their help in the dendrochronology laboratory. We would also like to thank Hydro-Québec for providing historical data on its powerline network and facilitating the logistics of fieldwork in the Eeyou Istchee James Bay administrative region. This work was funded by a Natural Science and Engineering Research Council (NSERC)-Alliance grant (PI: E. Thiffault; ALLRP 565308–21), by a NSERC Graduate Research Scholarship- Doctoral Program grant obtained by A. Harel in 2023 and by the Centre interdisciplinaire de recherche en opérationnalisation du développement durable and Fonds de recherche du Québec (Levier grant program; PI: E. Thiffault; 2020-RS4–265111). Part of the field work was paid by E. Thiffault (NSERC Discovery grant RGPIN-2018–05755).

Appendix A. Supporting information

Supplementary data associated with this article can be found in the online version at doi:10.1016/j.foreco.2026.123650.

Data availability

Research Link Provided.

References

Albrecht, A., Hanewinkel, M., Bauhus, J., Kohnle, U., 2012. How does silviculture affect storm damage in forests of south-western Germany? Results from empirical modeling based on long-term observations. Eur. J. For. Res. 131, 229–247. https://doi.org/10.1007/s10342-010-0432-x.

Bartoń, K., 2024. MuMIn: Multi-Model Inference.

Bates, D., Mächler, M., Bolker, B., Walker, S., 2015. Fitting linear mixed-effects models using lme4. J. Stat. Softw. 67, 1–48. https://doi.org/10.18637/jss.v067.i01.

Biondi, F., 1999. Comparing tree-ring chronologies and repeated timber inventories as forest monitoring tools. Ecol. Appl. 9, 216–227. https://doi.org/10.1890/1051-0761(1999)009%255B0216:CTRCAR%255D2.0.CO;2.

Black, B.A., Abrams, M.D., 2003. Use of boundary-line growth patterns as a basis for dendroecological release criteria. Ecol. Appl. 13, 1733–1749. https://doi.org/10.1890/02-5122.

Black, B.A., Abrams, M.D., 2004. Development and application of boundary-line release criteria. Dendrochronologia 22, 31–42. https://doi.org/10.1016/j.dendro.2004.09.004.

Boissonneault, D., Nielsen, S.E., 2025. Dynamics in tree structure and composition along boreal forest edges: a case study in Alberta's in situ oil sands. For. Ecol. Manag. 594, 122950. https://doi.org/10.1016/j.foreco.2025.122950.

Boucher, D., De Grandpré, L., Gauthier, S., 2003. Développement d'un outil de classification de la structure des peuplements et comparaison de deux territoires de la pessière à mousses du Québec. For. Chron. 79, 318–328. https://doi.org/10.5558/tfc79318-2.

Bowering, M., LeMay, V., Marshall, P., 2006. Effects of forest roads on the growth of adjacent lodgepole pine trees. Can. J. For. Res. 36, 919–929. https://doi.org/10.1139/x05-300.

Braithwaite, N.T., Mallik, A.U., 2012. Edge effects of wildfire and riparian buffers along boreal forest streams. J. Appl. Ecol. 49, 192–201.

Brassard, B.W., Chen, H.Y.H., Bergeron, Y., 2009. Influence of environmental variability on root dynamics in northern forests. Crit. Rev. Plant Sci. 28, 179–197. https://doi.org/10.1080/07352680902776572.

Briber, B.M., Hutyra, L.R., Reinmann, A.B., Raciti, S.M., Dearborn, V.K., Holden, C.E., Dunn, A.L., 2015. Tree productivity enhanced with conversion from forest to urban land covers. PLoS ONE 10, e0136237. https://doi.org/10.1371/journal.pone.0136237.

Bunn, A.G., 2008. A dendrochronology program library in R (dplR). Dendrochronologia 26, 115–124. https://doi.org/10.1016/j.dendro.2008.01.002.

Buras, A., 2017. A comment on the expressed population signal. Dendrochronologia 44, 130–132. https://doi.org/10.1016/j.dendro.2017.03.005.

Buss, J., Dabros, A., Higgins, K.L., Hammond, H.E.J., Pinzon, J., Langor, D.W., 2024. Comparison of edge effects from well pads and industrial roads on mixed upland boreal forest vegetation in Alberta. Plant Ecol. 225, 331–343. https://doi.org/10.1007/s11258-023-01393-3.

Chen, J.M., 1996. Optically-based methods for measuring seasonal variation of leaf area index in boreal conifer stands. Agric. For. Meteorol. 80, 135–163. https://doi.org/10.1016/0168-1923(95)02291-0.

Chen, J., Franklin, J.F., Spies, T.A., 1992. Vegetation responses to edge environments in old-growth Douglas-fir forests. Ecol. Appl. 2, 387–396.

De Schrijver, A., Devlaeminck, R., Mertens, J., Wuyts, K., Hermy, M., Verheyen, K., 2007. On the importance of incorporating forest edge deposition for evaluating exceedance of critical pollutant loads. Appl. Veg. Sci. 10, 293–298.

Désaulniers, G., 1998. Note de recherche forestière no90 - Aire de projection pour la cime d'un arbre. Gouvernement du Québec, Ministère des ressources naturelles, Direction de la recherche forestière.
Eldegard, K., Totland, Ø., Moe, S.R., 2015. Edge effects on plant communities along power line clearings. J. Appl. Ecol. 52, 871–880.
Esseen, P.-A., Hedström Ringvall, A., Harper, K.A., Christensen, P., Svensson, J., 2016. Factors driving structure of natural and anthropogenic forest edges from temperate to boreal ecosystems. J. Veg. Sci. 27, 482–492. https://doi.org/10.1111/jvs.12387.
Fortin, M., Lavoie, J.-F., Régnière, J., Saint-Amant, R., 2022. A Web API for weather generation and pest development simulation in North America. Environ. Model. Softw. 157, 105476. https://doi.org/10.1016/j.envsoft.2022.105476.
Franklin, C.M.A., Filicetti, A.T., Nielsen, S.E., 2021. Seismic line width and orientation influence microclimatic forest edge gradients and tree regeneration. For. Ecol. Manag. 492, 119216. https://doi.org/10.1016/j.foreco.2021.119216.
Fraver, S., White, A.S., 2005. Identifying growth releases in dendrochronological studies of forest disturbance. Can. J. For. Res. 35, 1648–1656. https://doi.org/10.1139/x05-092.
Gascon, C., Williamson, G.B., da Fonseca, G.A.B., 2000. Receding forest edges and vanishing reserves. Science 288, 1356–1358. https://doi.org/10.1126/science.288.5470.1356.
Haddad, N.M., Brudvig, L.A., Clobert, J., Davies, K.F., Gonzalez, A., Holt, R.D., Lovejoy, T.E., Sexton, J.O., Austin, M.P., Collins, C.D., Cook, W.M., Damschen, E.I., Ewers, R.M., Foster, B.L., Jenkins, C.N., King, A.J., Laurance, W.F., Levey, D.J., Margules, C.R., Melbourne, B.A., Nicholls, A.O., Orrock, J.L., Song, D.-X., Townshend, J.R., 2015. Habitat fragmentation and its lasting impact on Earth's ecosystems. Sci. Adv. 1, e1500052. https://doi.org/10.1126/sciadv.1500052.
Hansen, M.C., Potapov, P.V., Moore, R., Hancher, M., Turubanova, S.A., Tyukavina, A., Thau, D., Stehman, S.V., Goetz, S.J., Loveland, T.R., Kommareddy, A., Egorov, A., Chini, L., Justice, C.O., Townshend, J.R.G., 2013. High-resolution global maps of 21st-century forest cover change. Science 342, 850–853. https://doi.org/10.1126/science.1244693.
Hanson, J.J., Stuart, J.D., 2005. Vegetation responses to natural and salvage logged fire edges in Douglas-fir/hardwood forests. For. Ecol. Manag. 214, 266–278. https://doi.org/10.1016/j.foreco.2005.04.010.
Harel, A., Thiffault, E., Paré, D., 2021. Ageing forests and carbon storage: a case study in boreal balsam fir stands. For. Int. J. For. Res. 94, 651–663. https://doi.org/10.1093/forestry/cpab021.
Harel, A., Thiffault, E., Paré, D., Hudon, R., Larochelle, M., Chavaillaz, Y., 2025. Soil CO2 and CH4 effluxes in powerline rights-of-way and their adjacent forests. Agric. For. Meteorol. 374, 110801. https://doi.org/10.1016/j.agrformet.2025.110801.
Harper, K.A., Butler, W., O'Handley, K., 2024a. Vegetation patterns across edges of bogs and lakes in spruce and hemlock forests of southwestern Nova Scotia. Plant Ecol. 225, 305–316. https://doi.org/10.1007/s11258-023-01364-8.
Harper, K.A., Lesieur, D., Bergeron, Y., Drapeau, P., 2004. Forest structure and composition at young fire and cut edges in black spruce boreal forest. Can. J. For. Res. 34, 289–302. https://doi.org/10.1139/x03-279.
Harper, K.A., Macdonald, S.E., 2011. Quantifying distance of edge influence: a comparison of methods and a new randomization method. Ecosphere 2, art94. https://doi.org/10.1890/ES11-00146.1.
Harper, K.A., Macdonald, S.E., Burton, P.J., Chen, J., Brosofske, K.D., Saunders, S.C., Euskirchen, E.S., Roberts, D.A., Jaiteh, M., Esseen, P.-A., 2005. Edge influence on forest structure and composition in fragmented landscapes. Conserv. Biol. 19, 768–782. https://doi.org/10.1111/j.1523-1739.2005.00045.x.
Harper, K.A., Macdonald, S.E., Mayerhofer, M.S., Biswas, S.R., Esseen, P.-A., Hylander, K., Stewart, K.J., Mallik, A.U., Drapeau, P., Jonsson, B.-G., 2015. Edge influence on vegetation at natural and anthropogenic edges of boreal forests in C anada and Fennoscandia. J. Ecol. 103, 550–562.
Harper, K.A., Yang, J.R., Dazé Querry, N., Dyer, J., Alves, R.S.C., Ribeiro, M.C., 2024b. Limited influence from edges and topography on vegetation structure and diversity in Atlantic Forest. Plant Ecol. 225, 361–371. https://doi.org/10.1007/s11258-023-01353-x.
Harris, N.L., Gibbs, D.A., Baccini, A., Birdsey, R.A., de Bruin, S., Farina, M., Fatoyinbo, L., Hansen, M.C., Herold, M., Houghton, R.A., Potapov, P.V., Suarez, D.R., Roman-Cuesta, R.M., Saatchi, S.S., Slay, C.M., Turubanova, S.A., Tyukavina, A., 2021. Global maps of twenty-first century forest carbon fluxes. Nat. Clim. Change 11, 234–240. https://doi.org/10.1038/s41558-020-00976-6.
Hartig, F., 2022. DHARMa: Residual Diagnostics for Hierarchical (Multi-Level / Mixed) Regression Models.
Holmes, R.L., 1983. Computer-assisted quality control in tree-ring dating and measurement. Tree Ring Bull. 43, 69–78.
Jackson, R.B., Canadell, J., Ehleringer, J.R., Mooney, H.A., Sala, O.E., Schulze, E.D., 1996. A global analysis of root distributions for terrestrial biomes. Oecologia 108, 389–411. https://doi.org/10.1007/BF00333714.
Jackson, R.S., Dennett, J.M., Nielsen, S.E., 2023. Effects of oil sands disturbances on shrub and tree structure along forest edges in Alberta's boreal forest. Can. J. For. Res 53, 642–653. https://doi.org/10.1139/cjfr-2023-0005.
Kobayashi, H., Ryu, Y., Baldocchi, D.D., Welles, J.M., Norman, J.M., 2013. On the correct estimation of gap fraction: how to remove scattered radiation in gap fraction measurements. Agric. For. Meteorol. 174–175, 170–183. https://doi.org/10.1016/j.agrformet.2013.02.013.
Kuznetsova, A., Brockhoff, P.B., Christensen, R.H.B., 2017. lmerTest package: tests in linear mixed effects models. J. Stat. Softw. 82. https://doi.org/10.18637/jss.v082.i13.
Lambert, M.C., Ung, C.H., Raulier, F., 2005. Canadian national tree aboveground biomass equations. Can. J. For. Res. 35, 1996–2018. https://doi.org/10.1139/x05-112.
Laurance, W.F., Goosem, M., Laurance, S.G.W., 2009. Impacts of roads and linear clearings on tropical forests. Trends Ecol. Evol. 24, 659–669. https://doi.org/10.1016/j.tree.2009.06.009.
Laurance, W.F., Laurance, S.G., Ferreira, L.V., Rankin-de Merona, J.M., Gascon, C., Lovejoy, T.E., 1997. Biomass collapse in amazonian forest Fragments. Science 278, 1117–1118. https://doi.org/10.1126/science.278.5340.1117.
Lenth, R.V., Bolker, B., Buerkner, P., Giné-Vázquez, L., Herve, M., Jung, M., Love, J., Miguez, F., Riebl, H., Singmann, H., 2024. emmeans: Estimated Marginal Means, aka Least-Squares Means.
Levasseur, A., Mercier-Blais, S., Prairie, Y.T., Tremblay, A., Turpin, C., 2021. Improving the accuracy of electricity carbon footprint: estimation of hydroelectric reservoir greenhouse gas emissions. Renew. Sustain. Energy Rev. 136, 110433. https://doi.org/10.1016/j.rser.2020.110433.
Li, Q., Liu, Z., Jin, G., 2022. Impacts of stand density on tree crown structure and biomass: a global meta-analysis. Agric. For. Meteorol. 326, 109181. https://doi.org/10.1016/j.agrformet.2022.109181.
Lüdecke, D., Ben-Shachar, M.S., Patil, I., Waggoner, P., Makowski, D., 2021. performance: an R package for assessment, comparison and testing of statistical models. J. Open Source Softw. 6.
Ma, J., Li, J., Wu, W., Liu, J., 2023. Global forest fragmentation change from 2000 to 2020. Nat. Commun. 14, 3752. https://doi.org/10.1038/s41467-023-39221-x.
McDonald, R.I., Urban, D.L., 2004. Forest edges and tree growth rates in the North Carolina Piedmont. Ecology 85, 2258–2266. https://doi.org/10.1890/03-0313.
Meeussen, C., Govaert, S., Vanneste, T., Calders, K., Bollmann, K., Brunet, J., Cousins, S. A.O., Diekmann, M., Graae, B.J., Hedwall, P.-O., Krishna Moorthy, S.M., Iacopetti, G., Lenoir, J., Lindmo, S., Orczewska, A., Ponette, Q., Plue, J., Selvi, F., Spicher, F., Tolosano, M., Verbeeck, H., Verheyen, K., Vangansbeke, P., De Frenne, P., 2020. Structural variation of forest edges across Europe. For. Ecol. Manag. 462, 117929. https://doi.org/10.1016/j.foreco.2020.117929.
Meeussen, C., Govaert, S., Vanneste, T., Bollmann, K., Brunet, J., Calders, K., Cousins, S. A.O., De Pauw, K., Diekmann, M., Gasperini, C., Hedwall, P.-O., Hylander, K., Iacopetti, G., Lenoir, J., Lindmo, S., Orczewska, A., Ponette, Q., Plue, J., Sanczuk, P., Selvi, F., Spicher, F., Verbeeck, H., Zellweger, F., Verheyen, K., Vangansbeke, P., De Frenne, P., 2021a. Microclimatic edge-to-interior gradients of European deciduous forests. Agric. For. Meteorol. 311, 108699. https://doi.org/10.1016/j.agrformet.2021.108699.
Meeussen, C., Govaert, S., Vanneste, T., Haesen, S., Van Meerbeek, K., Bollmann, K., Brunet, J., Calders, K., Cousins, S.A.O., Diekmann, M., Graae, B.J., Iacopetti, G., Lenoir, J., Orczewska, A., Ponette, Q., Plue, J., Selvi, F., Spicher, F., Sørensen, M.V., Verbeeck, H., Vermeir, P., Verheyen, K., Vangansbeke, P., De Frenne, P., 2021b. Drivers of carbon stocks in forest edges across Europe. Sci. Total Environ. 759, 143497. https://doi.org/10.1016/j.scitotenv.2020.143497.
Morgenroth, J., Nowak, D.J., Koeser, A.K., 2020. DBH distributions in America's Urban forests—an overview of structural diversity. Forests 11, 135.
Morreale, L.L., Thompson, J.R., Tang, X., Reinmann, A.B., Hutyra, L.R., 2021. Elevated growth and biomass along temperate forest edges. Nat. Commun. 12, 7181. https://doi.org/10.1038/s41467-021-27373-7.
Mourelle, C., Kellman, M., Kwon, L., 2001. Light occlusion at forest edges: an analysis of tree architectural characteristics. For. Ecol. Manag. 154, 179–192. https://doi.org/10.1016/S0378-1127(00)00624-1.
Nakagawa, S., Johnson, P.C.D., Schielzeth, H., 2017. The coefficient of determination R2 and intra-class correlation coefficient from generalized linear mixed-effects models revisited and expanded. J. R. Soc. Interface 14, 20170213. https://doi.org/10.1098/rsif.2017.0213.
Nemani, R.R., Keeling, C.D., Hashimoto, H., Jolly, W.M., Piper, S.C., Tucker, C.J., Myneni, R.B., Running, S.W., 2003. Climate-driven increases in global terrestrial net primary production from 1982 to 1999. Science 300, 1560–1563. https://doi.org/10.1126/science.1082750.
Nowacki, G.J., Abrams, M.D., 1997. Radial-growth averaging criteria for reconstructing disturbance histories from presettlement-origin oaks. Ecol. Monogr. 67, 225–249. https://doi.org/10.1890/0012-9615(1997)067%5B0225:RGACFR%5D2.0.CO;2.
Oksanen, J., Simpson, G.L., Blanchet, F.G., Kindt, R., Legendre, P., Minchin, P.R., O'Hara, R.B., Solymos, P., Stevens, M.H.H., Szoecs, E., Wagner, H., Barbour, M., Bedward, M., Bolker, B., Borcard, D., Carvalho, G., Chirico, M., De Caceres, M., Durand, S., Evangelista, H.B.A., FitzJohn, R., Friendly, M., Furneaux, B., Hannigan, G., Hill, Lahti, L., McGlinn, D., Ouellette, M.-H., Cunha, E., Smith, T., Stier, A., Braak, C.J.F.T., Weedon, J., Borman, T., 2025. vegan: Community Ecology Package.
Pan, Y., Birdsey, R.A., Phillips, O.L., Houghton, R.A., Fang, J., Kauppi, P.E., Keith, H., Kurz, W.A., Ito, A., Lewis, S.L., Nabuurs, G.-J., Shvidenko, A., Hashimoto, S., Lerink, B., Schepaschenko, D., Castanho, A., Murdiyarso, D., 2024. The enduring world forest carbon sink. Nature 631, 563–569. https://doi.org/10.1038/s41586-024-07602-x.
Peltola, H., Kellomäki, S., Väisänen, H., Ikonen, V.-P., 1999. A mechanistic model for assessing the risk of wind and snow damage to single trees and stands of Scots pine, Norway spruce, and birch. Can. J. For. Res. 29, 647–661. https://doi.org/10.1139/x99-029.
Pfeifer, M., Lefebvre, V., Peres, C.A., Banks-Leite, C., Wearn, O.R., Marsh, C.J., Butchart, S.H.M., Arroyo-Rodríguez, V., Barlow, J., Cerezo, A., Cisneros, L., D'Cruze, N., Faria, D., Hadley, A., Harris, S.M., Klingbeil, B.T., Kormann, U., Lens, L., Medina-Rangel, G.F., Morante-Filho, J.C., Olivier, P., Peters, S.L., Pidgeon, A., Ribeiro, D.B., Scherber, C., Schneider-Maunoury, L., Struebig, M., Urbina-Cardona, N., Watling, J.I., Willig, M.R., Wood, E.M., Ewers, R.M., 2017. Creation of forest edges has a global impact on forest vertebrates. Nature 551, 187–191. https://doi.org/10.1038/nature24457.
Phipps, R.L., Whiton, J.C., 1988. Decline in long-term growth trends of white oak. Can. J. For. Res. 18, 24–32. https://doi.org/10.1139/x88-005.

Pinheiro, J., Bates, D., DebRoy, S., Sarkar, D., Heisterkamp, S., Van Willigen, B., Maintainer, R., 2017. Package 'nlme.' Linear and nonlinear mixed effects models, version 3, 274.
Prévost, M., Dumais, D., DeBlois, J., 2016. Morphological response of conifer advance growth to canopy opening in mixedwood stands, in Quebec, Canada. Trees 30, 1735–1747. https://doi.org/10.1007/s00468-016-1404-7.
R Core Team, 2020. R: A language and environment for statistical computing.
Reinmann, A.B., Hutyra, L.R., 2017. Edge effects enhance carbon uptake and its vulnerability to climate change in temperate broadleaf forests. Proc. Natl. Acad. Sci. 114, 107–112. https://doi.org/10.1073/pnas.1612369114.
Reinmann, A.B., Smith, I.A., Thompson, J.R., Hutyra, L.R., 2020. Urbanization and fragmentation mediate temperate forest carbon cycle response to climate. Environ. Res. Lett. 15, 114036.
Remy, E., Wuyts, K., Boeckx, P., Ginzburg, S., Gundersen, P., Demey, A., Van Den Bulcke, J., Van Acker, J., Verheyen, K., 2016. Strong gradients in nitrogen and carbon stocks at temperate forest edges. For. Ecol. Manag. 376, 45–58. https://doi.org/10.1016/j.foreco.2016.05.040.
Remy, E., Wuyts, K., Van Nevel, L., De Smedt, P., Boeckx, P., Verheyen, K., 2018a. Driving factors behind litter decomposition and nutrient release at temperate forest edges. Ecosystems 21, 755–771. https://doi.org/10.1007/s10021-017-0182-4.
Remy, E., Wuyts, K., Verheyen, K., Gundersen, P., Boeckx, P., 2018b. Altered microbial communities and nitrogen availability in temperate forest edges. Soil Biol. Biochem. 116, 179–188. https://doi.org/10.1016/j.soilbio.2017.10.016.
Ries, L., Fletcher, R.J., Battin, J., Sisk, T.D., 2004. Ecological responses to habitat edges: mechanisms, models, and variability explained. Annu. Rev. Ecol. Evol. Syst. https://doi.org/10.1146/annurev.ecolsys.35.112202.130148.
Riitters, K., Wickham, J., Costanza, J.K., Vogt, P., 2016. A global evaluation of forest interior area dynamics using tree cover data from 2000 to 2012. Landsc. Ecol. 31, 137–148. https://doi.org/10.1007/s10980-015-0270-9.
Saucier, J.-P., Grondin, P., Robitaille, A., Gosselin, J., Morneau, C., Richard, P.J.H., Brisson, J., Sirois, L., Leduc, A., Morin, H., Thiffault, E., Gauthier, S., Lavoie, C., Payette, S., 2009. Écologie Forestière, in: Ordre des ingénieurs forestiers du Québec (Ed.), Manuel de Foresterie. Éditions MultiMondes, Québec, pp. 165–216.
Schmidt, M., Jochheim, H., Kersebaum, K.-C., Lischeid, G., Nendel, C., 2017. Gradients of microclimate, carbon and nitrogen in transition zones of fragmented landscapes – a review. Agric. For. Meteorol. 232, 659–671. https://doi.org/10.1016/j.agrformet.2016.10.022.
Searle, S.R., Speed, F.M., Milliken, G.A., 1980. Population marginal means in the linear model: an alternative to least squares means. Am. Stat. 34, 216–221. https://doi.org/10.1080/00031305.1980.10483031.
Skrzyszewski, J., Pach, M., 2020. The use of the slenderness coefficient in diagnosing wind damage risksActa Silvestria57724.
Smith, I.A., Hutyra, L.R., Reinmann, A.B., Marrs, J.K., Thompson, J.R., 2018. Piecing together the fragments: elucidating edge effects on forest carbon dynamics. Front. Ecol. Environ. 16, 213–221. https://doi.org/10.1002/fee.1793.
Spellerberg, I.F., Fedor, P.J., 2003. A tribute to Claude Shannon (1916–2001) and a plea for more rigorous use of species richness, species diversity and the 'Shannon–Wiener' Index. Glob. Ecol. Biogeogr. 12, 177–179. https://doi.org/10.1046/j.1466-822X.2003.00015.x.
Strayer, D.L., Power, M.E., Fagan, W.F., Pickett, S.T.A., Belnap, J., 2003. A classification of ecological boundaries. BioScience 53, 723–729. https://doi.org/10.1641/0006-3568(2003)053%255B0723:ACOEB%255D2.0.CO;2.
Thorpe, H.C., Astrup, R., Trowbridge, A., Coates, K.D., 2010. Competition and tree crowns: a neighborhood analysis of three boreal tree species. For. Ecol. Manag. 259, 1586–1596. https://doi.org/10.1016/j.foreco.2010.01.035.
Vanneste, T., Depauw, L., De Lombaerde, E., Meeussen, C., Govaert, S., De Pauw, K., Sanczuk, P., Bollmann, K., Brunet, J., Calders, K., Cousins, S.A.O., Diekmann, M., Gasperini, C., Graae, B.J., Hedwall, P.-O., Iacopetti, G., Lenoir, J., Lindmo, S., Orczewska, A., Ponette, Q., Plue, J., Selvi, F., Spicher, F., Verbeeck, H., Zellweger, F., Verheyen, K., Vangansbeke, P., De Frenne, P., 2024. Trade-offs in biodiversity and ecosystem services between edges and interiors in European forests. Nat. Ecol. Evol. 8, 880–887. https://doi.org/10.1038/s41559-024-02335-6.
Venäläinen, A., Zeng, H., Peltola, H., Talkkari, A., Strandman, H., Wang, K., Kellomäki, S., 2004. Simulations of the influence of forest management on wind climate on a regional scale. Agric. For. Meteorol. 123, 149–158. https://doi.org/10.1016/j.agrformet.2003.12.005.
Visser, H., van der Maaten-Theunissen, M., Maaten, E. van der, 2023. BAI BAI bias – an evaluation of uncertainties in calculating basal area increments from cores. Dendrochronologia 78, 126066. https://doi.org/10.1016/j.dendro.2023.126066.
Wang, Y., Titus, S.J., LeMay, V.M., 1998. Relationships between tree slenderness coefficients and tree or stand characteristics for major species in boreal mixedwood forests. Can. J. For. Res. 28, 1171–1183. https://doi.org/10.1139/x98-092.
Weathers, K.C., Cadenasso, M.L., Pickett, S.T., 2001. Forest edges as nutrient and pollutant concentrators: potential synergisms between fragmentation, forest canopies, and the atmosphere. Conserv. Biol. 15, 1506–1514.
West, B.T., Welch, K.B., Galecki, A.T., 2006. Linear Mixed Models: A Practical Guide Using Statistical Software, First ed. Chapman and Hall/CRC, New York.
Wickham, H., Chang, W., Henry, L., Pedersen, T.L., Takahashi, K., Wilke, C.O., Woo, K., Yutani, H., Dunnington, D., Brand, T. van den, Posit, P.B.C., 2020. ggplot2 (R 4.0.2). Title: Create Elegant Data Visualisations Using the Grammar of Graphics.
Wickham, H., François, R., Henry, L., Müller, K., Vaughan, D., Posit Software, PBC, 2023. dplyr: A Grammar of Data Manipulation.
Wigley, T.M., Briffa, K.R., Jones, P.D., 1984. On the average value of correlated time series, with applications in dendroclimatology and hydrometeorology. J. Appl. Meteorol. Climatol. 23, 201–213.
Willmer, J.N.G., Püttker, T., Prevedello, J.A., 2022. Global impacts of edge effects on species richness. Biol. Conserv. 272, 109654. https://doi.org/10.1016/j.biocon.2022.109654.
Wuyts, K., De Schrijver, A., Vermeiren, F., Verheyen, K., 2009. Gradual forest edges can mitigate edge effects on throughfall deposition if their size and shape are well considered. For. Ecol. Manag. 257, 679–687. https://doi.org/10.1016/j.foreco.2008.09.045.
Yang, G., Crowther, T.W., Lauber, T., Zohner, C.M., Smith, G.R., 2025. A globally consistent negative effect of edge on aboveground forest biomass. Nat. Ecol. Evol. https://doi.org/10.1038/s41559-025-02840-2.
Yang, B., Shaw, R.H., Paw, U, K.T., 2006. Wind loading on trees across a forest edge: a large eddy simulation. Agric. For. Meteorol. 141, 133–146. https://doi.org/10.1016/j.agrformet.2006.09.006.
Zeng, H., Peltola, H., Väisänen, H., Kellomäki, S., 2009. The effects of fragmentation on the susceptibility of a boreal forest ecosystem to wind damage. For. Ecol. Manag. 257, 1165–1173. https://doi.org/10.1016/j.foreco.2008.12.003.
Ziter, C., Bennett, E.M., Gonzalez, A., 2014. Temperate forest fragments maintain aboveground carbon stocks out to the forest edge despite changes in community composition. Oecologia 176, 893–902. https://doi.org/10.1007/s00442-014-3061-0.
Zuur, A.F., Ieno, E.N., Walker, N.J., Saveliev, A.A., Smith, G.M., 2009. Mixed effects modelling for nested data. In: Zuur, A.F., Ieno, E.N., Walker, N., Saveliev, A.A., Smith, G.M. (Eds.), Mixed Effects Models and Extensions in Ecology with R. Springer, New York, New York, NY, pp. 101–142.